

Material Characterization of Components and Assembled Behavior of a Composite Liner for Rehabilitation of Cast Iron Pressure Pipes

Michael Brown,¹ Amir Fam,¹ Ian D. Moore²

¹ Department of Civil Engineering, Ellis Hall, Queen's University, Kingston, Ontario K7L 3N6, Canada

² GeoEngineering Centre at Queen's-RMC, Ellis Hall, Queen's University, Kingston, Ontario K7L 3N6, Canada

Work is underway to determine the stability limit states for a cast in place composite liner system used to repair cast iron pressure water pipes. To establish its performance in bridging ring fractures, perforations, and other failures in the cast iron "host" pipe, it is important that the material characteristics of this composite liner be determined. This study characterizes the mechanical properties of this liner in both the longitudinal and circumferential directions, and develops a method to achieve this goal. A technique is developed to form the liner from its individual components and prepare coupons with end tabs. Test results for coupons oriented parallel to the axis of the pipe (i.e., in the longitudinal direction) agree well with those obtained from coupons cut from a liner exhumed from an actual field installation. Since the coupons formed in the laboratory are flat, the same technique is used to test the liner in the hoop (or circumferential) direction. Tensile strength and stiffness in the hoop direction are 45% higher than that in the longitudinal direction. Tests performed on the individual components of the liner are also reported, and these explain the bilinear stress-strain response. *POLYM. ENG. SCI.*, 48:1231-1239, 2008. © 2008 Society of Plastics Engineers

INTRODUCTION

Cast iron pipes have been used since the late 1800s to build water distribution systems. Up until the early 1970s, the majority of these systems were constructed using gray cast iron pipes [1]. Since then, ductile iron has replaced gray cast iron in the production of water main conduits on account of its versatility and enhanced performance [2]. Nevertheless, there is increasing concern about the remaining service life of aging water distribution systems.

Due in a large part to corrosion and mechanical action, the structural integrity of old cast iron water pipes is in question [3]. Over the years, several failure modes have been observed, including wedge splitting, spiral cracking, longitudinal cracking, and circumferential breaks.

Currently, 90% of the repair work performed on water pipes is performed by the conventional method of digging an open trench and replacing the damaged pipe segment with a new one [4]. This procedure involves a great deal of work, requires a significant amount of time, and is often very costly. It can also be disruptive to the public and to traffic, especially in heavily populated urban areas. Moreover, Luk [5] states that this technique (i.e., replacing an old cast iron pipe with a new ductile or cast iron pipe) does not provide a permanent solution to the problem, since the corrosion process will start over again as soon as the new pipe is installed. To combat this internal corrosion process, damaged water mains (partially and fully deteriorated) are being lined using a variety of techniques. The American Water Works Association categorizes these lining techniques into three groups in their manual M28 Second Edition [6] on water main rehabilitation: nonstructural (Class I), semistructural (Class II/III), and structural (Class IV). Most spray lining techniques such as cement-mortar and epoxy lining are considered to be nonstructural and require the host pipe to be structurally sound. Thin-walled polyethylene liners such as those studied by Boot and coworkers [7, 8] are usually installed when the host pipe is still structurally sound, though they can maintain stability when perforations develop in the host pipe. Both of these liner types have limitations, however, since they block existing service connections and are not designed to maintain the pipeline once the old pipe structure is no longer able to withstand the internal fluid pressures.

Using state-of-the-art trenchless technology, a novel method involving a cured-in-place polymer pipe liner (CIPP) has been developed by Sanexen Environmental Services Inc. to structurally rehabilitate damaged cast iron

Correspondence to: Ian D. Moore; e-mail: moore@civil.queensu.ca
Contract grant sponsor: Natural Sciences and Engineering Research Council of Canada (through a Strategic Research Grant "Sustaining Urban Pipe Infrastructure Using Liners").
DOI 10.1002/pen.20975
Published online in Wiley InterScience (www.interscience.wiley.com).
© 2008 Society of Plastics Engineers

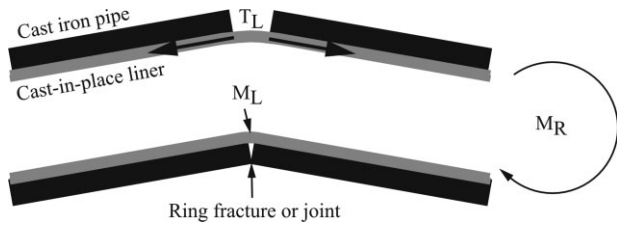


FIG. 1. Limit state 4: Moment and wall stretching at ring fracture/joint, after Allouche and Moore [14].

water mains [9]. This composite liner is designed to withstand the internal fluid pressure without assistance from the old pipe, and incorporates a technique for reopening service connections. The liner is composed of two concentric, tubular, plain-woven polyester jackets, with the inner jacket having a bonded layer of polyurethane elastomer on its inner surface. A polymeric resin is injected within the two jackets and the liner is pulled into place through an entry pit using a cable-winch system that is set up at a second access pit further along the section of pipe to be lined. It is then cured in the field using pressurized hot water. After curing, the service connections to lateral pipes are reopened using a remote-controlled robot. In addition to providing structural support for the damaged cast iron host pipe, the liner protects against further internal corrosion, helps maintain the pipe's hydraulic capacity, and prevents leakage.

RESEARCH SIGNIFICANCE

There has been a significant amount of research conducted on the application of CIPP liners in gravity flow pipes [10, 11]; however, to date there has been no significant research on applying the CIPP system in pressure pipe applications. As such, there are no ASTM guidelines for designing a CIPP liner in pressure pipe applications. ASTM F 1216-06 and ASTM F 1743-96(2003) are the only design standards used to date [12, 13]. However, the standard primarily focuses on calculation of design thickness of the CIPP liner for gravity flow pipes. F 1216 contains an equation for thickness of pressure pipe liners based on simple hoop resistance to internal pressure.

There is no discussion of other potential failure modes that may occur for pressure pipe liners.

This paper reports on an investigation of the constitutive characteristics of the composite pressure pipe liner. Specimens of the liner exhumed from a trial lining project undertaken in Hamilton (Ontario) are tested, as are the individual components of the liner in their precured states. Tensile tests have been performed in the longitudinal and circumferential directions on flat liner samples prepared in the laboratory. Comparisons are made between test results for the laboratory "replicas" and the samples exhumed from the field, to establish whether the in-house fabrication process provides representative samples.

The constitutive data from this study is being used to undertake finite element modeling of the cured in-place composite liner, so that limit states design methods can be developed for these structures. In particular, limit states 4 and 6 as defined by Allouche and Moore [14] are of interest (Figs. 1 and 2). These limit states are concerned with the overall bending moment or local bending moment and stretching force in the liner wall at ring fractures or joints (limit state 4), and local stresses associated with the liner in the vicinity of a water service connection (limit state 6). To address these properly, it is essential that the liner characteristics in the longitudinal and circumferential directions be determined.

EXPERIMENTAL PROCEDURES

The following sections provide details of the experimental program in terms of preparation and testing of various types of test specimens. This includes specimens exhumed from the field pipes and those fabricated in the laboratory, along with specimens of the individual components of the liner. Details of the testing procedures and instrumentation are also given.

Preparation of Specimens From the Exhumed Composite Liner

Figure 3 shows a cross-section of the lined cast iron pipe received from the field. The liner was extracted from the cast iron host pipe and cut into segments ~300 mm in

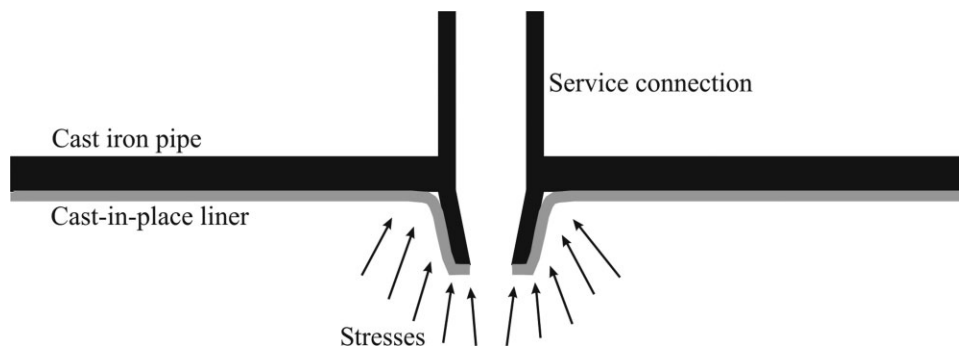


FIG. 2. Limit state 6: Stresses surrounding a service connection.

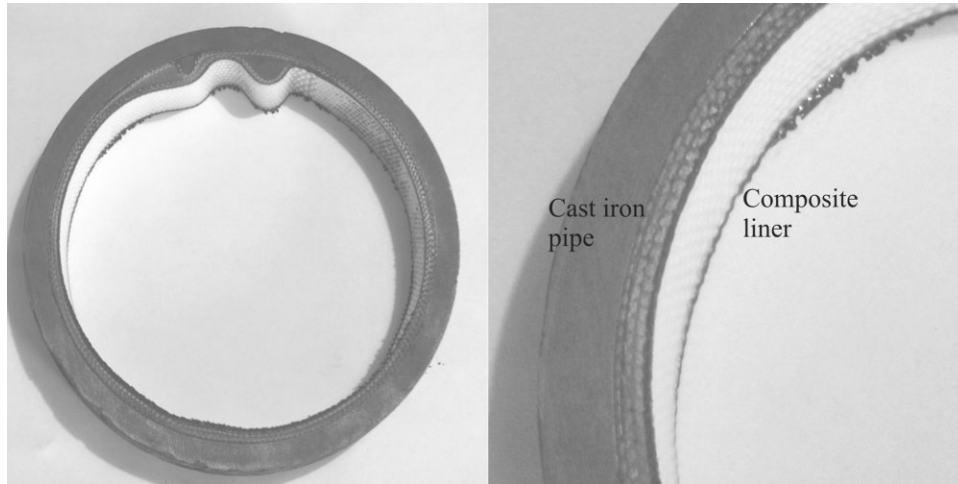


FIG. 3. Cross-section of exhumed cast iron pipe as received.

length. The outer diameter of the liner was 155 mm and the mean thickness was 4.7 mm, varying from a minimum of 4.51 mm to a maximum of 4.81 mm. Rectangular coupons, 25 mm × 225 mm, were cut along the longitudinal axis of the extracted tubular liner. Special glass fiber reinforced polymer (GFRP) tabs were fabricated to facilitate gripping of the coupons in the testing machine and also to conform to the curved surfaces of the coupons in the transverse direction, as shown in Fig. 4. The tabs consisted of glass fiber woven fabric, Tyfo SHE-51A, impregnated by Tyfo S Epoxy resin. After the epoxy-wetted fabric was installed on the two sides of the coupons, at both ends, the assembly was put between two parallel flat surfaces under ~30 kg of weights and left to cure for at least 48 h. Figure 5 shows a picture of the finished coupon, with the 50-mm long tabs installed at each end. Since no standards exist on testing this type of liners, the procedures used for preparation of fiber reinforced polymer (FRP) flat coupons (ASTM D 3039/3039M-00) was adopted here [15]. In total, seven coupons were prepared.

Preparation of Specimens From the Individual Components of the Composite Liner

The composite liner consists of inner and outer jackets, which are saturated with resin. The inner and outer jackets are essentially the same, except that the inner jacket has a nonstructural polyurethane elastomer layer bonded to its inner surface which is suitable for potable water. Sections of the inner and outer jackets were provided in their original form (i.e., woven polyester fiber fabric), as shown in Fig. 6a and b. Test coupons of the same dimensions as those prepared earlier (Fig. 5) were prepared from the inner and outer jackets, but in both the longitudinal and transverse directions. Additional coupons were made from the outer jacket in the longitudinal direction, with the circumferential strands removed from the fabric to examine their contribution and assess the effect of the plain weave. GFRP gripping tabs of the same type as described earlier were fabricated at the ends of these coupons. In total, 14 and 7 coupons were prepared from the outer jacket in the longitudinal and transverse directions,

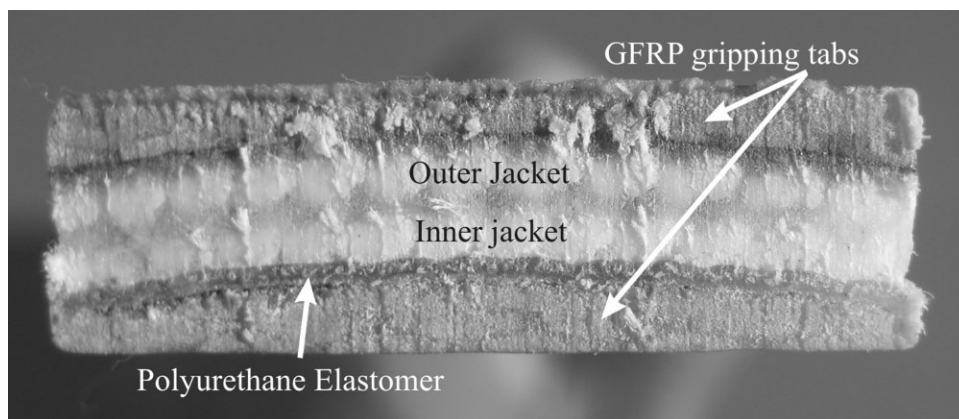


FIG. 4. End view of exhumed liner coupon.

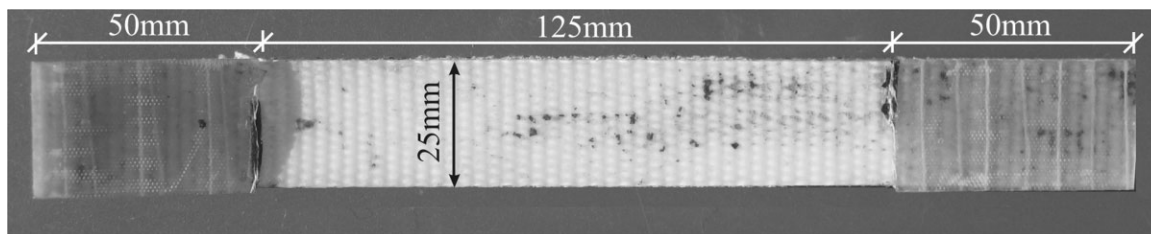


FIG. 5. Exhumed liner coupon with gripping tabs attached.

respectively, and 7 coupons were prepared from the inner jacket in each direction, longitudinal and transverse.

To make coupons from the resin, a type IV dumbbell cutting tool in accordance with ASTM D 638-03 [16] was used to create a mold out of a smooth, high-quality, high-density polyethylene geomembrane. This type of mold was suitable, since the cured resin did not adhere to the geomembrane and it was capable of retaining its form even at high curing temperatures. The resin coupons were made using three sheets of geomembrane stacked one on top of the other, with only the middle sheet cut to the dumbbell shape to act as the mold. After mixing the epoxy resin and hardener with the same ratio as used in the field (100:30 by weight), it was poured into the mold and pressed under ~ 30 kg of weights. The stack was then placed in a forced air oven and the resin was cured for ~ 1 h. This resulted in coupons made entirely of the curable polymeric resin. The first set of coupons was cured at 55°C , which is the approximate temperature of the hot water typically used in the field under pressure to inflate and cure the liner. To examine the effect of curing temperature, additional resin coupons were prepared and cured at temperatures of 20, 40, and 70°C . In total, five coupons were prepared for each curing temperature.

Preparation of the Specimen of In-House Fabricated Composite Liner

As the primary load on the liner is internal pressure, it is crucial to understand its behavior in the circumferential direction and establish its tensile strength and modulus in this direction. Flat uniaxial test specimens cannot be prepared from the exhumed cured liner to determine the constitutive characteristics in the hoop direction since the liner is curved. It was therefore decided to fabricate flat coupons of the composite liner in the hoop direction. To establish confidence in the validity of this technique to represent the behavior in the hoop direction, additional coupons representing the longitudinal direction were fabricated using the same technique and were used to compare the behavior in the longitudinal direction with that observed from the coupons cut from the exhumed liner (those discussed in the previous subsection).

A section of the precured liner consisting of the inner and outer jackets was cut into flat sheets as shown in Fig.

6a. Resin was poured in between the inner and outer jackets, and a rolling pin was used to saturate them with the resin. The wet system was then placed in between two geomembrane sheets and cured at a temperature of 55°C for 1 h. Approximately 30 kg of weights were set on top of the sheets to imitate the pressure that is applied in the field by the hot water when curing the liner. The fabricated composite liner was then removed from the oven and let sit for a day. Rectangular coupons of the same dimensions as those of the exhumed liner coupons were cut in both the longitudinal and transverse (representing the circumferential) directions. To maintain consistency,

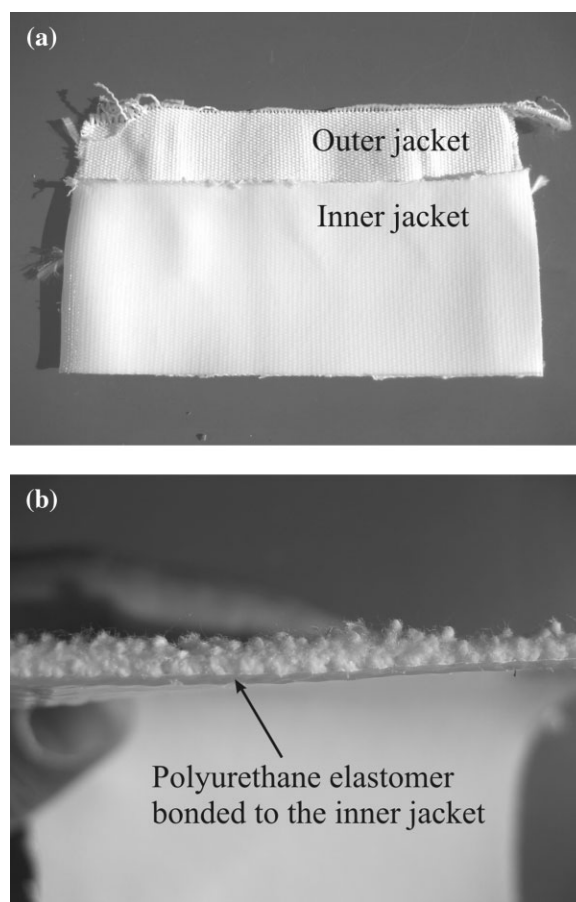


FIG. 6. (a) Inner and outer jackets of the composite liner. (b) Close-up of the inner jacket.

TABLE 1. Extensometer removal loads and mean maximum load.

Coupon type	Orientation	Extensometer removal load (N)	No. of coupons used in calculation of mean	Mean maximum load (N)	Standard deviation (N)
Exhumed liner	Longitudinal	6,000	4	7,884	87
Fabricated liner	Longitudinal	6,000	5	7,638	359
	Circumferential	7,750	5	10,170	591
Inner jacket	Longitudinal	3,000	5	3,956	177
	Circumferential	3,000	5	4,918	457
Outer jacket	Longitudinal	2,750	5	3,182	197
	Longitudinal strands	2,750	4	3,137	323
	Circumferential	2,750	5	5,176	281
Resin	Homogeneous	Not removed		—	

GFRP gripping tabs were also fabricated on the ends of the coupons even though the samples did not possess curvature. In total, seven coupons were fabricated in each of the longitudinal and transverse directions.

Experimental Setup and Instrumentation

A Zwick/Roell material testing machine was used to perform direct uniaxial tensile tests on all of the coupons. This is a tabletop test machine with a maximum load capacity of 20 kN. It is equipped with wedge grips and a longstroke extensometer that is accurate up to 5 μm . Although the extensometer has a robust construction and an impact-resistant measuring system, its arms were unclamped from the coupons at specified loads prior to failure, except when testing the resin coupons. Two coupons of each type were tested without the extensometer to estimate the maximum load of each type of coupon and to determine the removal loads of the extensometer. This was a precautionary measure to avoid any damage to the extensometer during the tests. All tests were performed at $23^\circ\text{C} \pm 1^\circ\text{C}$ (room temperature), and the rate of loading for each test was 5 mm/min.

RESULTS AND DISCUSSION

The data and graphs presented in this section are based on averaged values of five tests for each type of coupon. An “x” was placed in the tables where data were not available or inconclusive. Table 1 shows the loads at which the extensometer was unclamped from the different types of coupons. It also shows the mean maximum load that each group of coupons attained.

Behavior of the Individual Liner Components

The Polymeric Resin. The effect of curing temperature on the stress–strain behavior of the resin was investigated by curing the resin at four different temperatures. Figure 7 shows the stress–strain curves of the resin at the different curing temperatures. The data from 0% to 2% strain, where the behavior is generally linear, was used to calculate the elastic modulus of each resin coupon. A mean

modulus was then assessed at each curing temperature. Table 2 shows the tensile strength and modulus for each set of coupons along with the average values and standard deviations. There are no values for the tensile strength of the coupons cured at 70°C , because they all failed prematurely due to air bubbles. However, each sample was tested beyond the yield point, and so data for the tensile modulus were still available. The variation of tensile strength and modulus with curing temperature is given in Fig. 8. The strength and modulus of the cured resin increased with an increase in curing temperature but only up to 55°C , beyond which no increase in mechanical properties is observed. More tests may be needed for samples cured at temperatures higher than 70°C to verify this trend. A 28% increase in resin strength is seen from 20°C to 55°C . These tests confirm that a minimum amount of heat is required to allow the crosslinking reaction to take place during the curing process.

The smallest of imperfections was sufficient to cause the resin coupons to fail prematurely before the ultimate tensile strength was reached. This problem occurred most often with coupons that were cured at higher temperatures and when air bubbles existed. Multiple coupons were tested

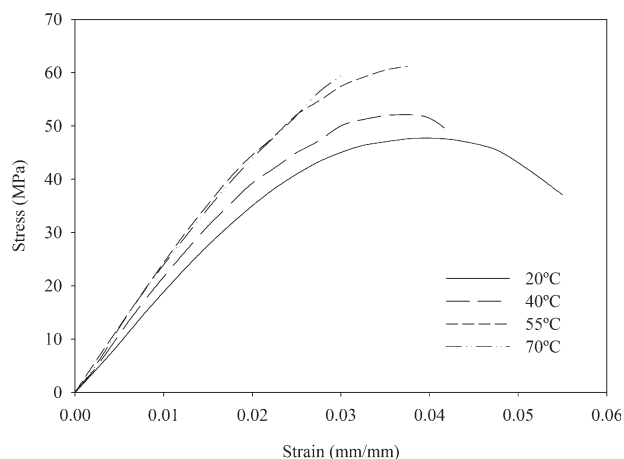


FIG. 7. Stress–strain curves for the resin coupons at various curing temperatures.

TABLE 2. Effect of curing temperature on the modulus and strength of the resin.

Curing temperature (°C)	Tensile modulus (MPa) (from 0% to 2% strain)			Tensile strength (MPa)		
	No. of coupons used in calculation of mean	Mean	Standard deviation	No. of coupons used in calculation of mean	Mean	Standard deviation
20	5	1832	162	3	47.5	0.6
40	5	2076	90	2	52.7	0.8
55	5	2356	133	2	60.8	0.6
70	4	2307	117	0	x	x

at each temperature until five provided data past the yield point, and these are the results that are presented.

The Inner and Outer Jackets. Figures 9 and 10 show the load–strain behavior of the inner and outer woven fabric jackets, respectively, in the longitudinal and hoop directions. The measured load is presented in Newton per millimeters, having divided the total load by the initial width of each specimen. Table 3 provides the mean ultimate load and tensile modulus along with standard deviations. Figure 9 shows that the inner jacket behaves linearly in both the longitudinal and circumferential directions, with tensile moduli of ~588 N/mm and 1530 N/mm, respectively. Figure 10 shows that the coupons cut from the outer jacket in the longitudinal direction follow a bilinear, strain-hardening curve. The initial modulus is ~200 N/mm and the final modulus is ~830 N/mm. This effect is caused by the plain-weave of the polyester fibers within the outer jacket. As the coupon elongates, the longitudinal strands straighten out and a stiffening effect takes place. This is seen at about 15–20% strain. The final modulus is relatively close in value to the modulus of the longitudinal coupons with the circumferential strands removed (980 N/mm), also shown in Fig. 10, because with the circumferential strands removed the tests begin with the strands almost fully elongated.

For both the inner and outer jackets, the tests performed in the circumferential direction show higher stiffness (1530 and 2270 N/mm, respectively) when compared with the tests performed in the longitudinal direction.

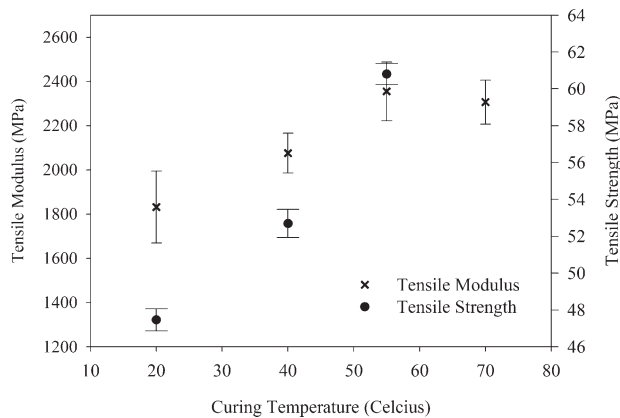


FIG. 8. Variation of tensile modulus and strength vs. curing temperature.

Behavior of the Exhumed Versus Fabricated Composite Liner

The longitudinal coupons cut from the composite liner fabricated in the laboratory produced very similar stress–strain curves to those cut from the exhumed liner as shown in Fig. 11. The liners behave linearly from 0% to 1% strain and again from 4% to 8% strain. However, they go through a stiffening phase between 8% and 9% strain, after which their moduli remain linear until the extensom-

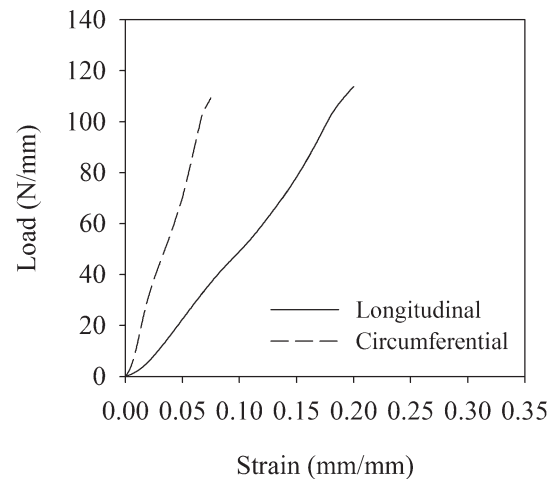


FIG. 9. Load–strain behavior of the inner jacket in the longitudinal and circumferential directions.

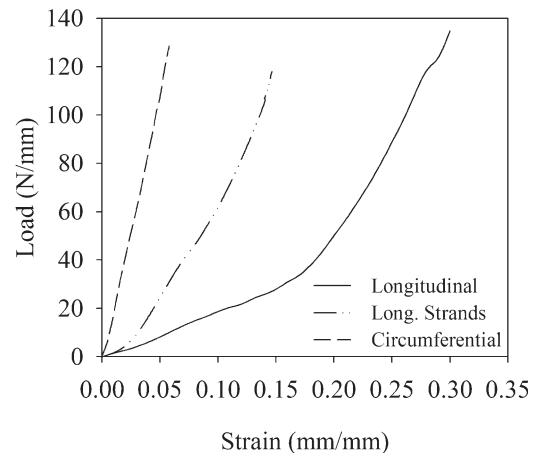


FIG. 10. Load–strain behavior of the outer jacket in the longitudinal and circumferential directions.

TABLE 3. Test results of the inner and outer jackets tested separately.

Coupon type	Orientation	No. of coupons used in calculation of mean	Tensile modulus (N/mm)		Ultimate load (N/mm)	
			Mean	Standard deviation	Mean	Standard deviation
Inner jacket	Longitudinal	5	588	31	154	6
	Circumferential	5	1530	90	182	11
Outer jacket	Longitudinal	5	194; 833	13; 28	161	9
	Longitudinal strands	4	982	82	167	13
	Circumferential	5	2270	56	242	18

eter is removed at a load of 6000 N, corresponding to stress of 49 MPa. The average ultimate tensile strengths of the exhumed and fabricated liners in the longitudinal direction are 61 MPa and 61.3 MPa, respectively. The ultimate tensile strengths were used to extrapolate both curves to estimate the strain at failure, which was ~21% for both liners. However, the maximum strain from a short-term test of this kind does not likely have significance, since liner design is generally based on ultimate stress rather than ultimate stain. All of the data presented in Table 4 were measured and not taken from the extrapolated portion of the curves.

The similarity in behavior of the longitudinal coupons prepared in the laboratory and those exhumed from the field provides credibility and a high level of confidence in the technique developed to produce test coupons in the laboratory. As such, test results of the artificially prepared coupons in the transverse direction are considered representative of the actual liner behavior in the circumferential direction. Figure 12 shows the average stress–strain curve of these coupons. It is clear that the composite liner is much stiffer and stronger in the hoop direction than in the longitudinal direction. The yield strain is approximately half the value of that in the longitudinal direction, but yield strength is similar in both orientations. The ultimate tensile strength in the circumferential direction (88.3

MPa) is ~45% higher than in the longitudinal direction. As before, the ultimate tensile strength was used to estimate the maximum hoop strain, which was found to be ~11%. The overall behavior and shape of the stress–strain curve in the circumferential direction is similar to that of the longitudinal direction. As summarized in Table 5, the initial modulus is the highest (3.04 GPa), followed by a significant postyield reduction (0.48 GPa) and then a slight increase up to 0.72 GPa to the point where the extensometer is removed at 7750 N, corresponding to a stress of 67 MPa.

By examining the overall behavior of the composite liner, shown in Figs. 11 and 12, and considering the behavior of the individual components (i.e. the resin and inner and outer jackets), shown in Figs. 7, 9, and 10, respectively, several key aspects of the liner’s behavior were noted. Initially, the resin dominates the behavior and contributes most of the stiffness of the system. The behavior eventually becomes nonlinear as a result of the stress–strain characteristics of the resin. As the resin becomes more nonlinear, load begins to transfer from the

TABLE 4. Comparison of the exhumed liner and the fabricated liner in the longitudinal direction.

Liner type	No. of coupons used in calculation of mean	Mean	Standard deviation
Exhumed			
Modulus (MPa)			
0–1%	4	2019	8.6
4–8%	4	115	14.8
9–13%	4	180	8.5
Yield strain (%)		1.0 ^a	
Yield strength (0.2% offset)		23.5 ^a	
Ultimate tensile strength (MPa)	4	61	0.6
Fabricated (longitudinal)			
Modulus (MPa)			
0–1%	5	2017	243
4–8%	5	135	15
9–13%	5	190	8
Yield strain (%)		0.9 ^a	
Yield strength (0.2% offset)		24 ^a	
Ultimate tensile strength (MPa)	5	61.3	2.8

^a These values were taken from the “average” curve of the test data (Fig. 11).

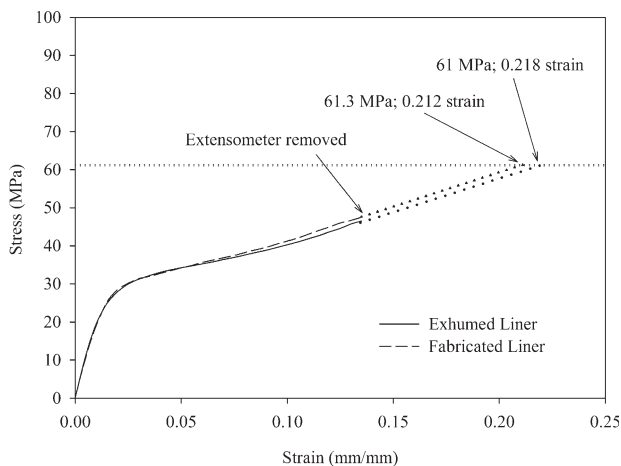


FIG. 11. Stress–strain curves for the exhumed and fabricated liners in the longitudinal direction.

resin to the inner and outer jackets, until the resin cracks at a strain of ~ 0.03 – 0.04 . From this point on, most of the load is carried by the jackets. However, the resin may continue to provide some of the overall stiffness through intact sections between the cracks. The behavior continues to be linear in the second part of the curve but at a substantially reduced modulus, reflecting the stiffness of the jackets.

SUMMARY AND CONCLUSIONS

The stress–strain behavior of the composite liner is generally bilinear, with a curved transition zone followed by strain-hardening behavior. The initial modulus and ultimate tensile strength in the hoop direction are $\sim 45\%$ higher than in the longitudinal direction. Since no specific standard currently exists for testing this type of material, an experimental methodology and a test specimen configuration based on ASTM D 3039/D 3039M-00 for glass and carbon FRPs have been adopted and resulted in successful tests. The ability to fabricate flat, composite liner sections from individual components in the laboratory has been established, and these resulted in a behavior almost identical to that obtained from exhumed liners that were cured in the field. The tensile strength of the liner in the hoop direction has been established and can be used in design to calculate the ultimate internal pressure of a circular axisymmetric liner using basic mechanics. It was also shown that the higher the curing temperature of the resin, the higher its strength and stiffness, up to a temperature of $\sim 55^\circ\text{C}$.

Additional research is needed to examine a number of effects. First, wrinkles typically occur in the liner when its diameter is slightly larger than that of the host pipe and this may have a substantial effect on the liner behavior. Second, the effect of rate of loading and cyclic loading on liner behavior should be investigated. Third, the effect of sustained loading and the long-term response of the liner needs to be examined.

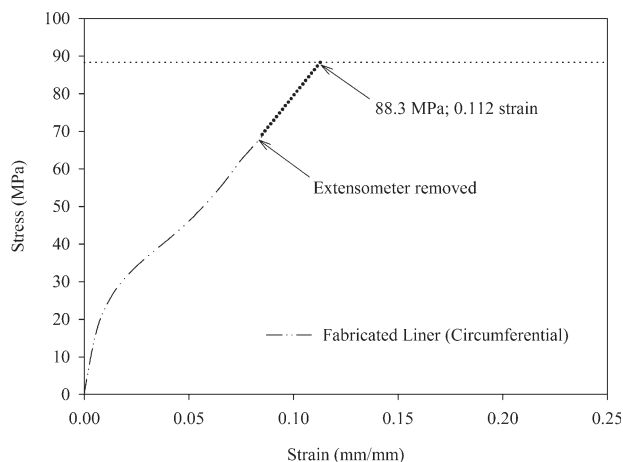


FIG. 12. Stress–strain curve for the fabricated liner in the circumferential direction.

TABLE 5. Data for the fabricated liner in the circumferential direction.

Fabricated (circumferential)	No. of coupons used in calculation of mean	Mean	Standard deviation
Modulus (MPa)			
0–0.5%	5	3040	120
2–5%	5	480	30
6–8%	5	720	75
Yield strain (%)		0.9 ^a	
Yield strength (0.2% offset)		24 ^a	
Ultimate tensile strength (MPa)	5	88.4	4.7

^a These values were taken from the “average” curve of the test data (Fig. 12).

ACKNOWLEDGMENTS

Liner samples were provided by Mr. Kevin Bainbridge of the City of Hamilton, Ontario, and samples of resin and fabrics were supplied by representatives from Sanexen Environmental Services Inc. and Fer-Pal Construction Ltd. The authors also appreciate Siddhartha Kumar Mandal for his work on fabricating the original coupons used for these tests.

REFERENCES

- M.V. Seica, J.A. Packer, M.W.F. Grabinsky, and B.J. Adams, *Can. J. Civil Eng.*, **29**, 2 (2002).
- R. Warda, *Ductile Iron Data for Design Engineers*, revised edition, Rio Tinto Iron & Titanium Inc., Section II, Montreal, Quebec (1990).
- M.V. Seica and J.A. Packer, *J. Mater. Civil Eng.*, **16**, 1 (2004).
- J.K. Jeyapalan, “Future of America’s Water Is in our Hands,” in *Proceedings of the ASCE International Conference on Pipeline Engineering and Construction: New Pipeline Technologies, Security and Safety*, June 13–16, 2, 1026 (2003).
- G.K. Luk, *J. Infrastruct. Syst.*, **7**, 3 (2001).
- M.E. Grahek, et al., *AWWA Manual 28. Rehabilitation of Water Mains, 2nd ed.* American Water Works Association, Denver, CO (2001).
- J.C. Boot, Z.W. Guan, and I. Toropova, *Trenchless Technol. Res.*, **11**, 1 (1996).
- J.C. Boot and I.L. Toropova, *Trenchless Technol. Res.*, **14**, 2 (1999).
- E.N. Allouche, K. Bainbridge, and I.D. Moore, *Laboratory Examination of a Cured in Place Pressure Pipe Liner for Potable Water Distribution System, paper D-03-04, No-Dig 2005*, Orlando, FL, 10 (2005).
- I.D. Moore and K. El-Sawy, *Transport. Res. Record*, **1541**, 127 (1996).
- K. El-Sawy and I.D. Moore, “Parametric Study for Buckling of Liners: Effect of Liner Geometry and Imperfections,” in

Proceedings of the 1997 ASCE Conference on Trenchless Pipeline Projects, June 8–11, 416 (1997).

12. ASTM F 1216-06, "Standard Practice for Rehabilitation of Existing Pipelines and Conduits by the Inversion and Curing of a Resin-Impregnated Tube," ASTM International, West Conshohocken, PA, www.astm.org (2006).
13. ASTM F 1743-96, "Standard Practice for Rehabilitation of Existing Pipelines and Conduits by Pulled-in-Place Installation of Cured-in-Place Thermosetting Resin Pipe (CIPP)," ASTM International, West Conshohocken, PA, www.astm.org (2003).
14. E.N. Allouche, K. Bainbridge, and I.D. Moore, *Laboratory Examination of a Cured in Place Pressure Pipe Liner for Potable Water Distribution System, paper D-3-04, No-Dig 2005*, North American Society of Trenchless Technology, Orlando, FL (2005).
15. ASTM D 3039/3039M-00, "Standard Test Method of Tensile Properties of Polymer Matrix Composite Materials," ASTM International, West Conshohocken, PA, www.astm.org (2006).
16. ASTM D 638-03, "Standard Test Method for Tensile Properties of Plastic," ASTM International, West Conshohocken, PA, www.astm.org (2003).